Process Safety and Environmental Protection 105 (2017) 303–315

Contents lists available at ScienceDirect

Process Safety and Environmental Protection

journal homepage: www.elsevier.com/locate/psep

# Transesterification activity and characterization of natural CaO derived from waste venus clam (*Tapes belcheri* S.) material for enhancement of biodiesel production

O.N. Syazwani[a,b], Siow Hwa Teo[a,b,c], Aminul Islam[a,e], Yun Hin Taufiq-Yap[a,b,c,d,*]

[a] Catalysis Science and Technology Research Centre, Faculty of Science, Universiti Putra Malaysia, 43400 UPM Serdang, Selangor, Malaysia
[b] Department of Chemistry, Faculty Science, Universiti Putra Malaysia, 43400 UPM Serdang, Selangor, Malaysia
[c] Materials Synthesis and Characterization Laboratory, Institute of Advanced Technology, Universiti Putra Malaysia, 43400 UPM Serdang, Selangor, Malaysia
[d] Curtin Sarawak Research Institute, Curtin University, Miri, Sarawak, Malaysia
[e] Faculty of Engineering, Universiti Malaysia Sabah, 88400 Kota Kinabalu, Sabah, Malaysia

ARTICLE INFO

*Article history:*
Received 26 March 2015
Received in revised form 7 November 2016
Accepted 9 November 2016
Available online 17 November 2016

*Keywords:*
Heterogeneous catalyst
Waste *Tapes belcheri*
Recycled calcium carbonate
Transesterification
Correlation of basic sites
Biodiesel

ABSTRACT

In this study, waste venus clam (WVC) was used as a raw materials of catalyst to produce biodiesel from palm oil at atmospheric pressure. The thermogravimetric, surface functional group, morphology, structure, basicity, surface area and leaching properties of catalyst was studied by using TGA, FTIR, SEM, XRD, TPD-$CO_2$, BET, and AAS respectively. The result demonstrated that CS-900 catalyst gave high amount of total basicity at about 44 times than commercial CaO catalyst which is favorable for higher catalytic activity. Further, it was evident from BET that the shells calcined in temperature range 800–900 °C was exhibited enhance surface area than uncalcined shells. Under the best reaction condition (temperature 65 °C, methanol/oil molar ratio 15:1, reaction time 6 h, and catalyst 5 wt.% of oil), a high biodiesel yield of 97% was obtained. The leaching test on synthesized biodiesel revealed that the concentration of Ca in the biodiesel was 1.214 ppm which is inacceptable levels of metals as ASTM D6751 (United State) and in Europe, EN 14214 (Europe) standards. The subsequent reuse of the catalyst indicates the viability of utilizing waste shell as green catalysts for synthesis of biodiesel.



## 1. Introduction

Based on the Goldman Sachs report (Goldman, 2003; Sieferle, 1982), fossil fuels supplies are no longer as infinite as they encounter problems in terms of energy security, economic security and environmental security (Juan et al., 2011). The costly price of diesel fuel and rapid oil depletion of crude oil reserves that leading to search for alternative sources energy. Renewable fuels *i.e.* liquids (biodiesel and bioethanol) and gases were posed an alternative development partway for many fuel developers. Thus, the sustainable and renewable fuel should be easily available, environmental friendly and techno-economically competitive (Juan et al., 2011; Abdullah et al., 2009).

Biodiesel has appeared as one of the most potential renewable energy to substitute current petrol-derived diesel. Biodiesel, also called

* *Corresponding author at*: Catalysis Science and Technology Research Centre, Faculty of Science, Universiti Putra Malaysia, 43400 UPM Serdang, Selangor, Malaysia. Fax: +60 3 89466758.
E-mail address: taufiq@upm.edu.my (Y.H. Taufiq-Yap).
http://dx.doi.org/10.1016/j.psep.2016.11.011
0957-5820/

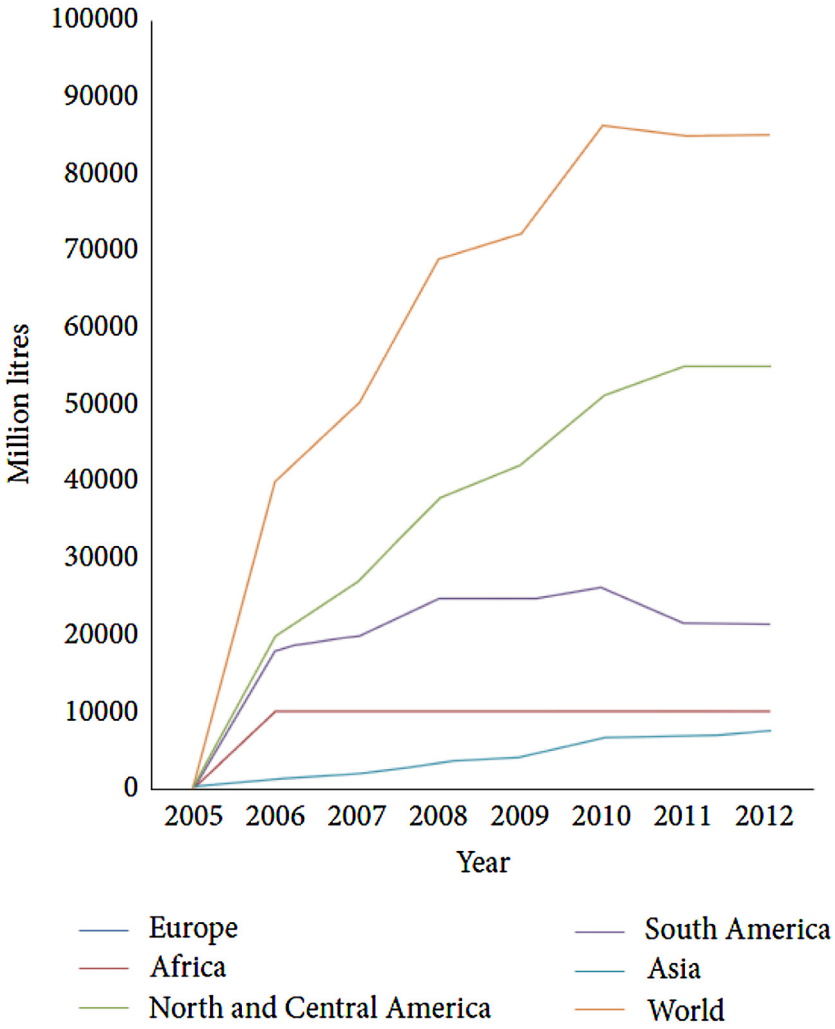


**Fig. 1 – Production of biodiesel (Gnanaprakasam et al., 2013).**

lower alkyl esters of long chain fatty acids or fatty acid methyl esters (FAMEs), which are produced through transesterification of triglycerides from vegetable oils or animal fats, in the presence of a short chain alcohol (usually methanol) and a catalyst (Sbihi et al., 2014; Sharma and Singh, 2010). The worldwide biodiesel production has grown sharply (Fig. 1) as it is renewable, nontoxic, bio-degradable, with low exhaust emission, excellent lubricity, and carbon neutral (Gnanaprakasam et al., 2013; Islam et al., 2013a; Knothe et al., 2005; Sharma et al., 2010a). The physicochemical and fuel properties of biodiesel are grouped into the same range as petroleum diesel hence; biodiesel can be used in unmodified diesel engine. Additionally, it can also be applied to a variety of others applications as a fuel in aviation, surfactant and heating oil (Sbihi et al., 2014).

The major obstacle to biodiesel commercialization is its high cost, which is approximately 1.5 times higher than petroleum diesel fuel due to the reaction processes and catalyst used (Juan et al., 2011; Islam et al., 2013a). One of the best ways to reduce the cost of biodiesel is to increase biodiesel yield production. Thus, the reaction temperature, catalyst amount, reaction time, and methanol/oil molar ratio are essential parameters in industrial level of biodiesel production (Islam et al., 2013a; Sharma et al., 2010b). Typically, catalystic reactions used are alkali catalyzed, acid catalyzed and enzymatic transesterification whereby they achieved the best results in biodiesel production. Other than enzymatic one, those alkaline and acid catalyzed are performed in the presence of homogeneous catalysts, *i.e.* NaOH, KOH and $H_2SO_4$ (Kouzu et al., 2008; Teo et al., 2015). The main concern is the downstream treatment cost which required multi-purification and water washing to remove soluble homogeneous catalyst. Moreover, the yield of the final biodiesel product was reduce during separation and washing step. Therefore, homogeneous transesterification reaction is not a feasible approach to be employed in the current industrial commercialization purposes as this conventional process reduce the production efficiency and high production cost.

Alternatively, heterogeneous catalytic process overcomes the homogeneous one since the solid catalysts can be easily recovered and potentially be reusable (Shajaratun et al., 2014; Islam et al., 2013b; Taufiq-Yap et al., 2014). Furthermore, biodiesel can be produced at a lower temperature with an alkali catalyst, while acid catalysts require a higher temperature and longer reaction time (Dmytryshyn et al., 2004; Vicente et al., 2004). Hence, utilization of solid catalysts instead of homogeneous catalysts could potentially lead to cheaper production costs and make the total cost of biodiesel production is competitive to the cost of petroleum diesel. Among the heterogeneous catalysts, calcium oxide (CaO) is an environment-friendly material has been used as a promising heterogeneous catalyst in transesterification reaction (Kouzu et al., 2008; Granados et al., 2007; Liu et al., 2008).

Generally, $Ca(NO_3)_2$, $CaCO_3$, or $Ca(OH)_2$ is the raw material to produce CaO catalysts (Cho et al., 2009). Unfortunately, the preparation of the highly effective solid catalysts is complex, costly, and requires experienced people to operate it (Wei et al., 2009). The fabricating cost of catalyst could be a important factor in its industrial applications. Thus, the production of biodiesel calls for an efficient and cheap catalyst to make the process economic and fully ecologically friendly, accordingly reducing its price and making it competitive with petroleum diesel (Lee et al., 2009; Praful et al., 2012; Batista et al., 1999; Michael, 1992). To address this issues, the interest of using waste material (calcium carbonate) from several natural calcium sources as raw materials for catalyst synthesis *i.e.* mollusk shell (Boey et al., 2009), eggshell (Viriyaempikul et al., 2010), *Mereterix mereterix* (Praful et al., 2012), snail shell (Birla et al., 2012) and clam shell (Taufiq-Yap et al., 2012) could eliminate

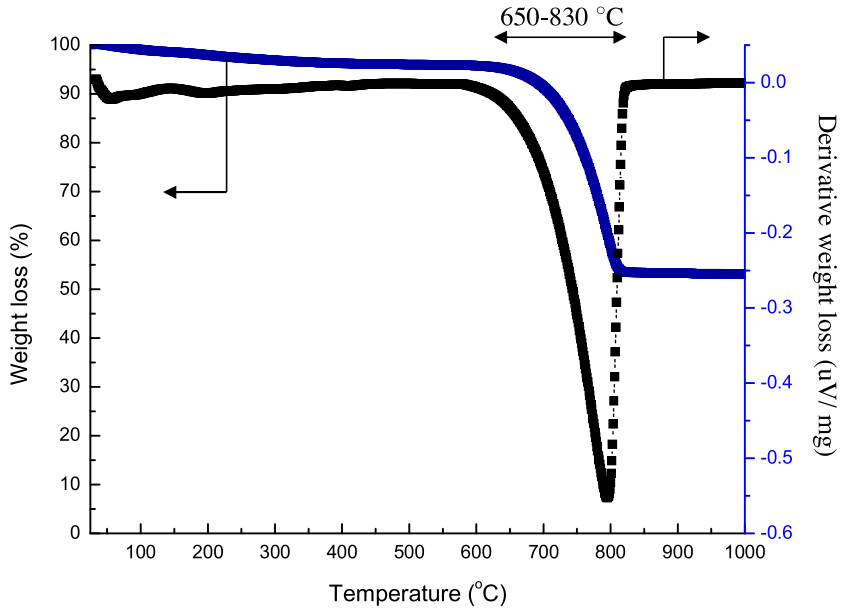


**Fig. 2 – TG/DTA profiles of WVC catalyst.**

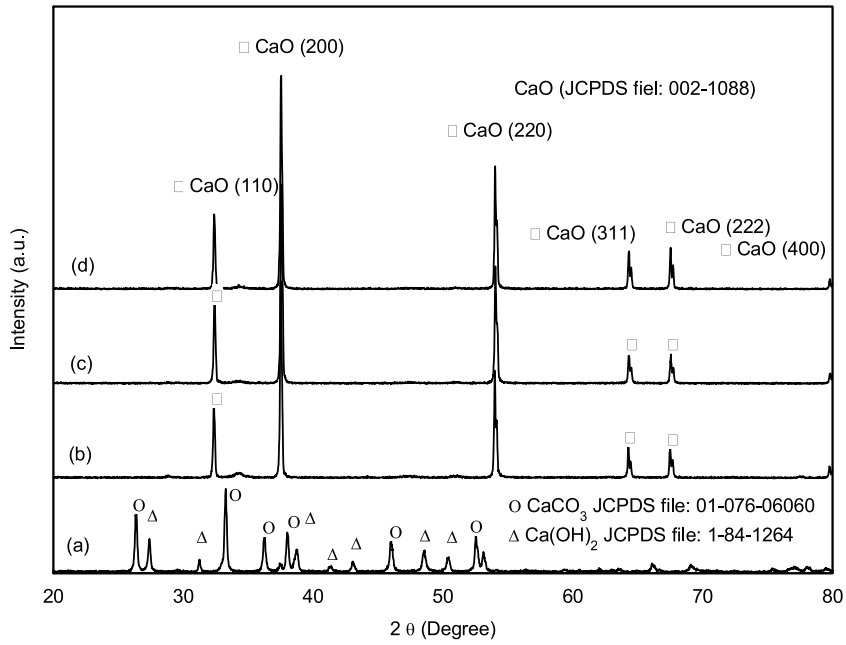


**Fig. 3 – X-ray diffraction patterns of WVC (a), CS-800 (b), CS-850 (c) and CS-900 (d) catalysts. ○ characteristic peak of $CaCO_3$, □ characteristic peak of CaO and Δ characteristic peak of $Ca(OH)_2$.**

the wastes and simultaneously produced an efficiency heterogeneous catalyst for transesterification.

Further study on the relationship between transesterification activity with surface basicity of calcined catalyst at various temperatures together with the reusability of the catalyst would be essentially useful for realizing this approach. Therefore, a study on the relationship between transesterification activity with surface basicity of calcined catalyst at various temperatures were investigated in this research. Moreover, the catalytic activity of *Meretrix venus* shell was investigated by various parameters, for example, molar ratio of methanol/oil, calcination time and calcination temperature of catalysts. Physicochemical properties of the developed catalysts has been characterized through thermo-gravimetric/differential thermal (TG/DTA) analysis, X-ray diffraction (XRD), Fourier transform infrared spectroscopic (FT-IR), Brunauer–Emmett–Teller (BET) surface area measurement and temperature programme desorption of carbon dioxide (TPD-$CO_2$).

## 2. Experimental

### 2.1. *Materials*

WVC shells were collected from a local market. Refined palm oil was obtained and used for this study. *n*-Hexane and methanol (reagent grade) were purchased from Fisher Scientific. Pure methyl ester standard mixture (mixture of 37 FAME components, Sigma–Aldrich) and internal standard (methyl heptadecanoate, ≥99%, Fluka Analytical) were used for quantification of FAME yield.

### 2.2. *Catalyst preparation*

The shells were cleaned by washing thoroughly with hot water several times to remove any organic impurity. Then they were

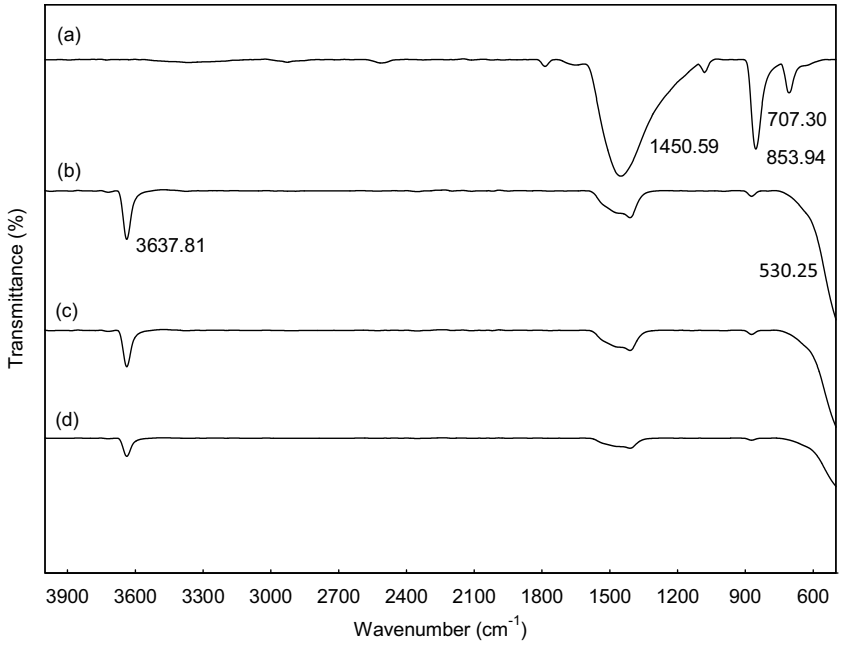


**Fig. 4 – FTIR spectra of WVC (a), CS-800 (b), CS-850 (c) and CS-900 (d) catalysts.**

dried overnight at 100 °C for 24 h. After drying, the shells were crushed using a pestle and mortar followed by grinding till it become powdered. It were then allowed to pass through a 0.8 mm sieve mesh. The powdered shell was then calcined at a different temperatures range from 800 to 900 °C for 6 h. The obtained solid products were denoted as CS-X, where X represented the increment calcination temperature of 800, 850 and 900 °C, respectively. Whereas the uncalcined waste shells were donated as WVC.

### 2.3. *Characterization techniques*

The WVC shells were analyzed by thermogravimetric/differential thermal (TG/DTA; Mettler Toledo model 990 Instrument) analyzer under nitrogen flow condition at temperature range from 25 to 1000 °C with 10 °C $min^{-1}$ of heating rate to determine phase transformation temperature. The crystalline phase of the samples were examined by X-ray diffraction (XRD; Shimadzu diffractor model XRD 6000) coupled with Cu K$\alpha$ radiation ($\lambda$ = 0.15,406 nm) at 30 kV, 15 mA in a scan range of 10–70°. The surface functional group of the samples were evaluated by Fourier transform infrared spectroscopy (FT-IR; Perkin Elmer 1650 Spectrometer) recorded in the range 400–4000 $cm^{-1}$. BET surface area were measured by a nitrogen adsorption/desorption analyzer ona Thermo Finnigan Sorptomatic 1990 series. The sample was degassed at 150 °C prior to analysis and the adsorption of nitrogen was measured at −196 °C. Total basic site and basicity strength distribution of catalysts were determined by TPD-$CO_2$ using Thermo Finnigan TPDRO 1100. This was carried out in a quartz tube packed with 50 mg of the sample. Pretreatment was done in nitrogen gas flow (20 ml $min^{-1}$) at 250 °C for 10 min (10 °C $min^{-1}$). The initial treatment was carried out with flow of $CO_2$ (flow rate of 30 ml $min^{-1}$) for 1.5 h and cooled to 50 °C. The nitrogen gas flow (20 ml $min^{-1}$) was again introduced for 30 min in order to remove excess $CO_2$ which presents in the system. Then, desorption of the chemisorbed $CO_2$ was performed by flowing helium gas flow from ambient temperature to 900 °C at heating rate of 10 °C $min^{-1}$. The surface structure was illustrated with a scanning electron microscope (SEM; JOEL). The catalysts were coated with gold using sputter coater.

**Table 1 – Crystallite size and BET surface area of WVC, short necked clam [12], *Meretrix venus* [11], golden apple snail [11], eggshell [11], CS-800, CS-850 and CS-900 catalysts.**

| | Catalyst | Crystallite sizes (nm)[a] | $S_{BET}$ ($m^2$ $g^{-1}$)[b] |
|---|---|---|---|
| (a) | Uncalcined | | |
| | Waste venus clam (WVC) | NA[c] | 2.8 ± 0.15 |
| (b) | Calcined | | |
| | Short necked clam | NA[c] | 0.6 |
| | *Meretrix venus* | NA[c] | 0.9 |
| | Golden apple snail | NA[c] | 0.9 |
| | Eggshell | NA[c] | 1.1 |
| | Commercial CaO | 66.3 ± 0.18 | 4.1 ± 0.50 |
| | CS-800[d] | 36.1 ± 0.15 | 9.5 ± 0.23 |
| | CS-850[d] | 39.4 ± 0.11 | 11.6 ± 0.19 |
| | CS-900[d] | 42.5 ± 0.21 | 7.5 ± 0.12 |

[a] Determined by using Debye–Scherrer equation.
[b] BET surface area.
[c] Not available.
[d] Current study.

### 2.4. *Catalytic activity*

For a typical reaction, the reactants were added into 100 ml round-bottom flask equipped with a reflux condenser and it was heated at 65 °C using oil bath under constant stirring rate of 600 rpm. Investigation on effect of catalyst dosage (1–6 wt.%), methanol/oil molar ratio (5–25 mol $mol^{-1}$) and reaction time (1–7 h) were carried out in order to achieve maximum biodiesel yield. Upon the completion of reaction, the product was collected at room temperature. Then, the catalyst and liquid layer were separated via centrifugation. The solid catalyst was removed and the oil liquid layer was go through vacuum drying process in a rotary evaporator to remove excess methanol. Reaction product was left overnight in a separating

**Table 2 – TPD-$CO_2$ profiles for commercial CaO, CS-800, CS-850 and CS-900 catalysts.**

| Catalyst | Peak temperature (°C) | $CO_2$ desorbed ($\mu$mol g$^{-1}$) |
|---|---|---|
| CS-900 | 707 | 13156.80 ± 4.30 |
| CS-850 | 650 | 801.26 ± 3.25 |
| CS-800 | 623 | 385.61 ± 2.11 |
| Commercial CaO | 611 | 294.20 ± 1.37 |

funnel to form upper and lower layers. The lower layer which is glycerol was drawn off and the remaining fatty acid methyl ester (FAME) on the upper layer was collected for further analysis.

### 2.5. *Biodiesel characterization*

Analysis of the fatty acid profile was carried out quantiticaly with a GS QP5050A series gas chromatograph (Shimadzu) equipped with flame ionization detector and coupled to a mass spectrometer (QP2010 Plus). A HP-5 column was used with He as a carrier gas. The oven temperature is isothermal at 320 °C and the injector and detector temperature was set to 280 °C. Mass spectra were acquired using MS software and peaks identification was supported with the NIST MS library. The observed mass range was set from 37 to 800 a.m.u. to remove the solvent. The methyl ester yield in biodiesel was analyzed by gas chromatography (GC) (Agilent technologies 7890A) with a FID (flame ionization detector) and a polar BP-20 capillary column with 30 m in length and 0.5 mm internal diameter was employed. It should be noted that the duplicate experiments were performed, and the errors of % FAME contents were typically within ±2.0 wt.%. The content of methyl ester was calculated according to European regulated procedure EN 14103. The yield of biodiesel was calculated by using Eq. (1) (Yang et al., 2009) as follows:

$$\text{Yield (\%)} = \frac{\text{weight of biodiesel produced}}{\text{weight of oil used}} \times 100 \quad (1)$$

### 2.6. *Reusability and leaching tests*

Reusability of catalyst was studied by collecting the remaining spent catalyst after each reaction, The spent catalysts were washed throughly with *n*-hexane and methanol, followed with reactivation temperature at 900 °C for 2 h. The reaction was carried out under optimized conditions. After the completion of transesterification, the biodiesel produced was analyzed by using atomic absorption spectrophotometer (AAS; Thermoscientific model S serial AA) to determine the leached active ion ($Ca^{2+}$) in the biodiesel.

**Table 3 – Fatty acid methyl ester compositions of the biodiesel synthesized from palm oil.**

| Peak | Free fatty acid composition | Retention time |
|---|---|---|
| 1 | Palmitic acid, C16:0 | 16.832 |
| 2 | Oleic acid, C18:1 | 18.823 |
| 3 | Linoleic acid, C18:0 | 19.151 |
| 4 | Lauric acid, C1:0 | 14.645 |

**Table 4 – Transesterification activities of WVS, Commecial CaO, CS800, CS850 and CS-900 catalysts for biodiesel production.**

| Catalysts | FAME yield (%) |
|---|---|
| WVC[b] | 5.21 ± 1.55 |
| Commecial CaO[a] | 64.23 ± 1.19 |
| CS-800[b] | 14.06 ± 2.18 |
| CS-850[b] | 14.32 ± 3.21 |
| CS-900[b] | 78.25 ± 2.84 |

[a] Transesterification condition: catalyst amount 5 wt.%, *n*(methanol):*n*(oil) = 15:1, reaction time 4 h, 65 °C reaction temperature.
[b] Transesterification condition: catalyst amount 5 wt.%, *n*(methanol):*n*(oil) = 10:1, reaction time 6 h, 65 °C reaction temperature.

## 3. Results and discussion

### 3.1. *Thermogravimetry analysis*

Fig. 2 depicts the thermograms of WVC shells analyzed by TG/DTA at ramp rate 10 °C min$^{-1}$. Only a single prominent step of weight loss of 42% was found for the sample at temperature 650–830 °C, corresponding to the decomposition of $CaCO_3$ to CaO, as confirmed by the result from XRD (Fig. 3) and the FTIR (Fig. 4) analysis. This also can attributed to the evolvement of $CO_2$ from $CaCO_3$ to give CaO. The weight of the sample remained constant at above 850 °C. Therefore, the temperature above 650 °C required to transformed $CaCO_3$ (calcite) to CaO as shown in Eq. (2) as following:

$$CaCO_3 \rightarrow CaO + CO_2 \quad (2)$$

From the result, suitable catalyst preparation temperature was chosen 800 °C to synthesize CaO from waste clam shells.

### 3.2. *Structural and crystallography*

Fig. 3 demonstrated the XRD patterns for uncalcined and calcined catalysts. All the calcined WVC catalysts showed identical, clear and sharp reflection peaks at 2$\theta$ of 37.22°, 53.57°, 64.24° and 67.49°, indicating to a single crystalline phase of CaO (JCPDS file no. 00-002-1088). The calcined WVC catalysts revealed different intensity of reflection peaks at different temperatures, illustrating the crystalline size of activated CaO phase was increased in the following order: CS-800 > CS-850 > CS-900. The shell calcined at 900 °C are narrower with higher reflection peaks intensity compared to those calcined at 800 and 850 °C. This is due to the well-crystallized structure of the catalyst at higher temperature that released more basic sites of catalyst (Islam et al., 2013b). The crystallite sizes of CS-800, CS-850 and CS-900 catalysts were calculated using Debye–Scherrer equation according to highest intensity reflection peak of CaO (Table 1). The result demonstrated that the crystallite size of CaO phase of CS-800, CS-850 and CS-900 with different calcination temperatures were smaller than commercial CaO.

On the other hand, small and low intensity diffraction peaks which are identical to $CaCO_3$ were detected for WVC shell. The reflection peaks (2$\theta$ = 26.30°, 32.25°, 36.37°, 38.48°, 45.87°, 52.89°) were the characteristic peaks of $CaCO_3$ corresponding to the JCPDS file no. 01-076-0606 based on compound aragonite. Meanwhile, weak diffraction peaks were detectable

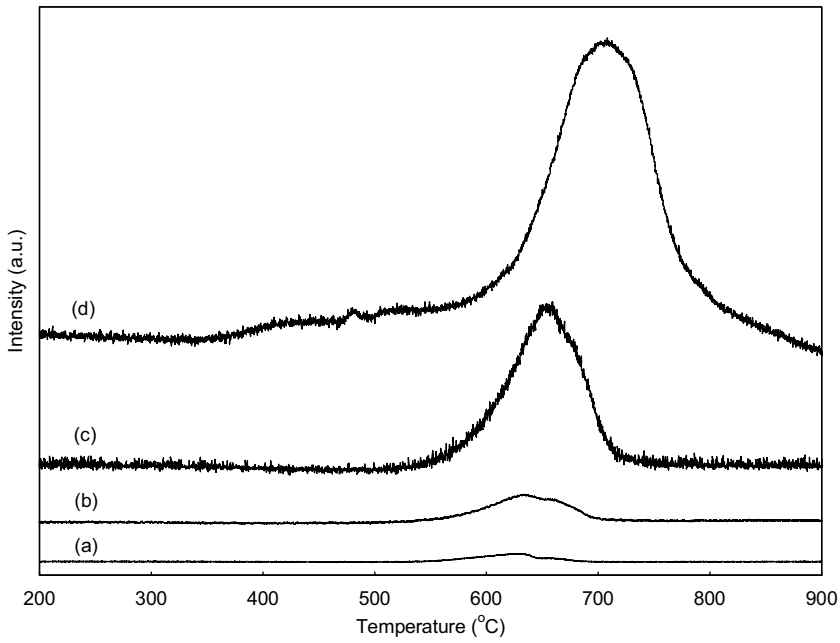


**Fig. 5 – TPD-$CO_2$ of CaO (a), CS-800 (b), CS-850 (c) and CS-900 (d) catalysts.**

for the present of $Ca(OH)_2$ in the natural waste material. It should be noted that the activated CaO was rapidly hydrated as shown in FT-IR spectrum (Fig. 4), and thus in order to prevent deterioration of the catalyst, it must be keep in desiccator to avoid any long exposure of the CaO with air.

### 3.3. *Functional groups*

The FT-IR spectra of uncalcined and calcined catalysts were illustrated in Fig. 4. The characteristic absorption peaks of WVC shell was observed from the spectrum indicated the asymmetric stretching (1450.59 $cm^{-1}$), out of plane bending (853.94 $cm^{-1}$) and in-plane bending vibration (707.30 $cm^{-1}$) modes, corresponding to $CO_3^{2-}$ group from $CaCO_3$. This result also observed from other calcium carbonate containing waste shells such as *Turbonilla striatula* and eggshell (Boro et al., 2011; Sharma and Singh, 2009).

Consequently, the IR spectra of the calcined catalysts (CS-800, CS-850 and CS-900) revealed an absorption band at 530 $cm^{-1}$ corresponding to CaO. There was no absorption band of $CO_3^{2-}$ group being observed indicated $CaCO_3$ in the clam shell was completely transformed to CaO. However, a small $OH^-$ absorption band (3637.81 $cm^{-1}$) was observed from the spectrum indicated that CaO can be hydrolyzed to $Ca(OH)_2$ by a prolonged exposure to open air. Hence, 900 °C is the most ideal calcination temperature to obtain a high purity CaO catalyst.

### 3.4. *Surface area and pore size*

The specific surface area of the uncalcined/calcined catalysts determined based on nitrogen adsorption/desorption isotherms are presented in Table 1. It showed that CS-800, CS-850 and CS-900 catalysts possesses a surface area of 9.5, 11.6 and 7.5 $m^2\,g^{-1}$, respectively. The results were in agreement with crystallite size of the catalyst (Table 1) whereby the higher surface area of catalyst possed the smaller crystallite size (Islam et al., 2013b). The calcined catalyst appeared to be higher surface area compared to the WVC catalyst of 2.8 $m^2\,g^{-1}$. The surface area was increased due to transformation of the composition in the sample during calcination process, which promoted a high surface area (Boro et al., 2011). However, the prolonged treatment and high temperature process would bring about the sintering of the catalyst (CS-900) concomitantly with large particle size and therefore the lowering of the surface area. Interestingly, all catalysts revealed the higher surface area compared to the sources reported (Viriya-empikul et al., 2010; Taufiq-Yap et al., 2012), which also included surface area of commercial CaO (4.1 $m^2\,g^{-1}$).

The pore sizes for WVC, CS-800, CS-850 and CS-900 catalysts were 2.9, 3.1, 8.5 and 5.8 nm, respectively. These showed that the pore size of the clam shell catalyst increased after calcination as well as BET surface area. The formation of pores in the catalyst prepared was caused by the evolution of gaseous carbonization products ($CO_2$ in this case) and partly due to the formation of CaO (Boro et al., 2011). A high porosity catalyst is a key requirement to achieve high conversion efficiency for heterogeneous process, thereby high surface areas or high catalytic sites are necessary.

### 3.5. *Basicity*

The catalyst basicity of commercial CaO, CS-800, CS-850 and CS-900 catalysts has been determined by $CO_2$ temperature programmed desorption as shown in Fig. 5. The total basicity of solid catalyst played main character as an active centers for transesterification reaction, as reported by Taufiq-Yap et al. (2012). A comparison was made with the commercial CaO. A small peak was obtained at 611 °C with total amount of basicity of 294.20 $\mu mol\,g^{-1}$ of $CO_2$ desorption. From the TPD-$CO_2$ results, clam shell derived catalysts gives high value of basicity compared to commercial CaO indicated that the catalyst can give higher catalytic activity. The results indicated that basicity of catalysts were in agreement with thermal decomposition temperature (Fig. 2) which increased of calcination temperature with the enhancement of basicity site of catalysts. The total amount of basicity for CaO, CS-800, CS-850 and CS-900 catalysts were shown in Table 2. It was found that total basicity of examined catalysts was arranged in the sequence of: CaO < CS-800 < CS-850 < CS-900. $CO_2$ desorption peaks temperature greater than 500 °C were due to the

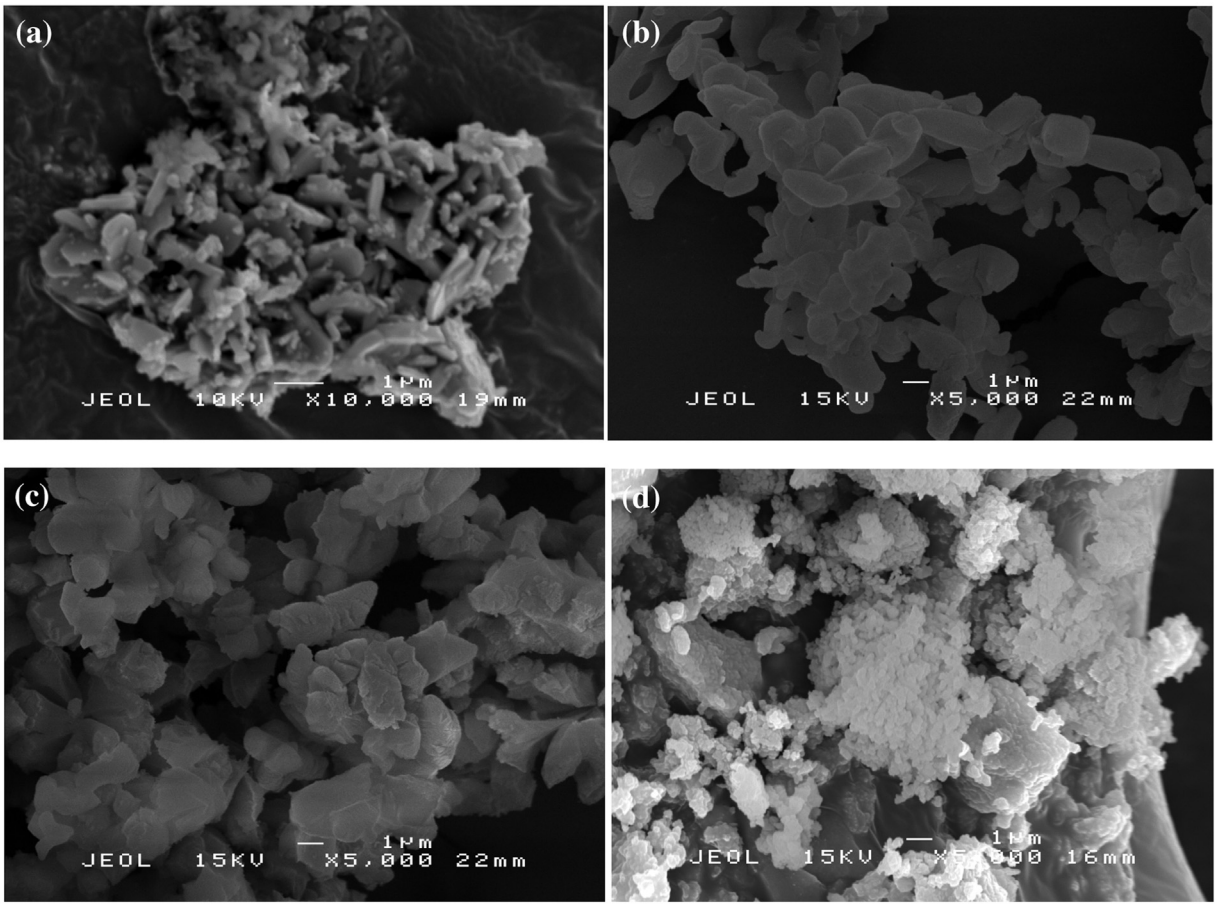


**Fig. 6 – Sem morphology of WVC (a), CS-800 (b), CS-850 (c) and CS-900 (d) catalysts.**

presence of strong interaction of $CO_2$ with super basic sites (Taufiq-Yap et al., 2012). One broad desorption peak of CS-900 catalyst was observed from an offset temperature (370–874 °C) and peak maximum at 707 °C with total amount of $CO_2$ desorption of 13,156.80 μmol $g^{-1}$. The result demonstrated that basicity of CS-900 catalyst with about 44 times higher than commercial CaO catalyst (294.20 μmol $g^{-1}$). The total basicity increased when the calcination temperature of the catalysts was raised from 800–900 °C. Decarbonation of $CaCO_3$ to form CaO catalyst rendered a high basicity. The surface lattice $O^{2-}$ ($Ca^{2+}$-$O^{2-}$) was attributed to Lewis base sites which favor for transesterification of triglycerides to fatty acid methyl esters (Viriya-empikul et al., 2010; Taufiq-Yap et al., 2012; Yang et al., 2009; Boro et al., 2011).

### 3.6. *Particle morphology and dimensions*

Morphology illustrations of WVS, CS-800, CS-850 and CS-900 catalysts were demonstrated in Fig. 6. Fig. 6(a) was exhibited big particles typically comprises the rod or plate-like shaped aragonite crystals clearly appeared in the natural WVS. SEM images of the as-synthesized catalysts (CS-800, CS-850 and CS-900) dipicted the presence of irregular shape with various sizes of particles after calcined at different temperatures (Fig. 6(b–d)). The WVS was decomposed and converted into $CO_2$ and CaO, smaller particles were obtained because a large amount of $CO_2$ escape from the system. This phenomenon supports the XRD result (Fig. 3). Fig. 6(b) clearly showed irregular shapes of agglomerated particles of CS-800 catalyst. the surface morphology of CS-800 catalyst was smooth, flat and nonporous in nature. In other word, the particle size should directly respond to the surface area. Whereas, the structural and morphology was turned into massive irregular particle shapes of calcium material as the major component when it calcined at 850 °C. The surface of CS-850 catalyst (Fig. 6(c)) was changed into rough, pitted and a number of visible voids were generated during the calcination. As a result, CS-850 (11.6 $m^2$ $g^{-1}$) catalyst had a higher surface area than CS-800 (9.5 $m^2$ $g^{-1}$) catalyst. When the temperature decomposition raise up to 900 °C, the CS-900 catalyst (Fig. 6(d)) was observed as clusters of particles which agglomerated from small particles. The agglomeration of small particles was lead to slightly reduced of specific surface area (7.5 $m^2$ $g^{-1}$) of catalyst, however, it is lower than surface area of CS-800 and CS-850 catalysts due to agglomeration and connection of many smaller particles from sintering effect at high calcination temperature (Shajaratun et al., 2014; Islam et al., 2013b; Taufiq-Yap et al., 2014).

### 3.7. *GC analysis of the biodiesel components*

The fatty acid methyl esters compositions of the biodiesel are given in Table 3 and the GC chromatogram is shown in Fig. 7. From the chromatogram, there are four major peaks were observed which corresponding to palmitic acid, oleic acid, linoleic acid and lauric acid, respectively. The composition fatty acid methyl esters are comparable with the EN 14103 and ASTM standards (Shajaratun et al., 2014; McNeff et al., 2008).

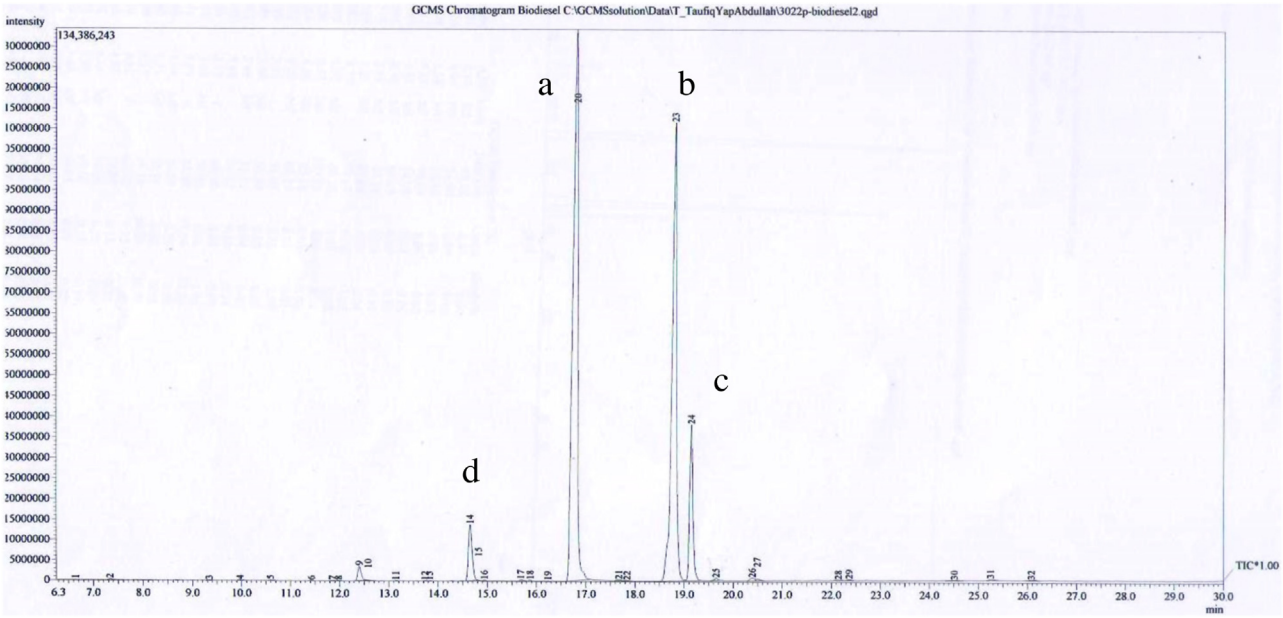


**Fig. 7 – GC-MS chromatogram of biodiesel produced using CS-900 catalyst. fatty acid compositions: palmitic acid (a), oleic acid (b), linoleic acid (c), lauric acid (d).**

### 3.8. *Effect of calcination temperature*

#### 3.8.1. *Correlation between basicity with FAME yield*

The effect of calcination temperature (800, 850 and 900 °C) on biodiesel yield over WVS, CS-800, CS-850 and CS-900 catalysts was investigated (Table 4). The conversion of palm oil was found non active for WVS catalyst with not produce biodiesel in the reaction. Furthermore, it was found that the shells calcined at 800 and 850 °C for 6 h were not enough to give highly active catalyst for transesterification reaction. Interestingly, calcined shell at 900 °C exhibited encouraging result in converting triglyceride to biodiesel throughout the reaction course with yield of 78%. This condition revealed CaO catalyst has an identical behavior since higher calcination temperature was needed for generating more basic site on the catalyst (Taufiq-Yap et al., 2012).

The correlation between the amount of basicity of the catalyst on transesterification reaction of oil was tested. Fig. 8 demonstrated the FAME conversion trend of catalysts with presence total basicity. This outcome was in good agreement with Taufiq-Yap et al. (2014) who mentioned that the higher basicity presence on catalyst enhances the catalytic activity on transesterification. In addition, the catalytic activity of CS-900 was optimized and compared with several calcium based catalysts (Table 5) on transesterification of oils. As can seen, calcium based catalysts derived from different waste shells (*Scylla serrata*, *Meretrix venus*, *Orbicularia orbiculata and Turbonilla striatula*) possed different catalytic performance. The studies revealed that these catalysts gave more than 90% of biodiesel yield. In this study, CS-900 catalyst was capable to render better FAME yield (97%) with low leaching (1.214 mg/L). The current prepared heterogeneous catalyst revealed better stability and sustainability.

#### 3.8.2. *Effect of reaction time*

The effect of reaction time on the transesterification activity of CS-900 catalyst was investigated at range of 1–7 h. As shown in Fig. 9, almost no FAME yield was formed at the initial first hour. The FAME yield increased when the reaction time was extended to 2 h (2%). Then, the FAME yield was started to increased to 22% at 5 h. At 6 h, the catalyst nearly completed the transesterification, reaction with yield of 97%.

In a heterogeneous catalytic system, the two reactants (tryglyceride and methanol) are immiscible at the beginning of the reaction results in low conversion rate for first 4 h with only 9% of yield. However, high FAME yield was due to the formation of mono and diglycerides that can facilitate the diffusion of the reactants and products (Totarat et al., 2006). Therefore, the absent of methyl ester content at the first hour and rapid increased in methyl ester content after 4 h suggested that the time required for formation of sufficient amount of these triglyceride derivatives. Nevertheless, the FAME yield decreased dramatically after prolongation of reaction to 7 h. This might designate that the transesterification reaction achieved equilibrium condition, additional proceeds of the reaction that may lead to the reverse of reaction to reactant side and consequently reduced the biodiesel content.

#### 3.8.3. *Effect of methanol to oil molar ratio*

The reaction were carried out with different methanol to oil molar ratios (5–25) to test the influence of methanol volume on the FAME yield and the results are given in Fig. 10. It can be seen that the yield attained was 78% at methanol/oil molar ratio of 10 wt.%. Upon increasing the ratio to 15 wt.%, the optimum FAME yield of 97% was achieved. The results suggested that the methanol ratio at 10 wt.% or below is insufficient to disperse oil and catalyst phase, and facilitate the transesterification. When the ratio was stoichiometrically increased to 15 wt.%, the mixture become more miscible, then driving the reaction towards methyl ester formation (Islam et al., 2013a; Shajaratun et al., 2014; Islam et al., 2013b; Taufiq-Yap et al., 2014). Nonetheless, the FAME yield remarkably reduced when the methanol/oil molar ratio added to 20 and 25 wt.%. Since the transesterification is reversible in nature, this result might be due to the reverse transesterification reaction (Shajaratun et al., 2014). When glycerin remains in the solution, it helps to shift back the equilibrium of the reaction to the left, the reverse reaction between glycerol and methyl ester promote to form the triglycerides derivatives *i.e.* monoglycerides and diglyc-

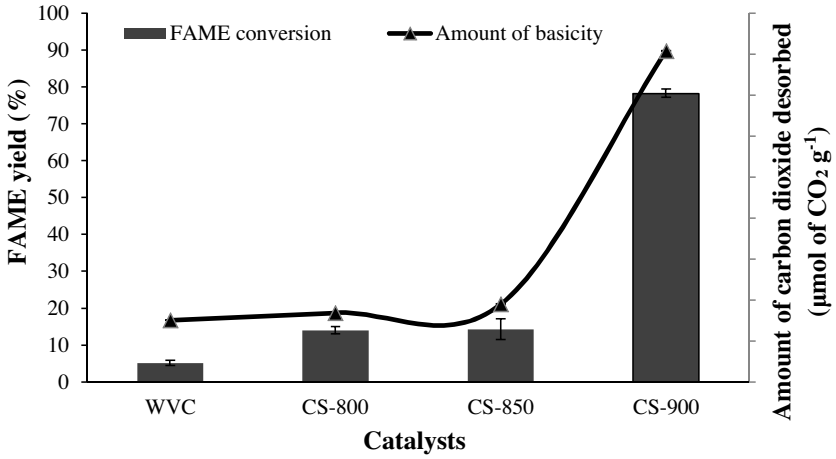


**Fig. 8 – Correlation between the total basicity and FAME conversion of the WVC, CS-800, CS-850 and CS-900 catalyst.**

**Table 5 – Summary of waste shell derived calcium based catalysts for transesterification reaction.**

| Catalyst | Synthesis method | Reaction parameters | Yield (%) | Reusability (time) | Leaching (mg/l) | Ref. |
|---|---|---|---|---|---|---|
| *Scylla serrata* | Decomposition at 900 °C for 2 h | 10 g of palm oil, methanol to oil molar ratio is 0.5, 5 wt.% of catalyst, 65 °C at 2.5 h | 90% | 11 | NT[a] | Boey et al. (2009) |
| *Meretrix venus* | Thermal decomposition at 800 °C in air | Palm olein oil (50 ml), 18:1 methanol to oil molar ratio, catalyst amount is 10 wt.% with reaction temperature at 60 °C for 2 h | 95% | NT[a] | NT[a] | Praful et al. (2012) |
| *Orbicularia orbiculata* | Activated at 900 °C for 3 h | Jatropha oil (13 wt.% of FFA content), methanol: oil ratio is 15:1 at 65 °C for 6 h | 93% | NT[a] | NT[a] | Taufiq-Yap et al. (2012) |
| *Turbonilla striatula* | Thermal decomposition at 900 °C in air | Commercial mustard oil (10 g), 3 wt.% of catalyst, 9:1 methanol to oil ratio and a reaction temperature 65 °C for 6 h | 93% | 2 (yield >80%) | NT[a] | Boro et al. (2011) |
| *Tapes belcheri* (CS-900) | Decarbonation at 900 °C for 6 h | Palm oil (10 g), methanol:oil ratio is 15:1, 5 wt.% of catalyst, 65 °C, 6 h | 97% | 3 (yield >95%) | 1.214[b] | Current study |

[a] NT = Not tested.
[b] Determined by AAS analysis.

erides (Fig. 11), and lowering the yield of esters (Murugesan et al., 2009).

### 3.8.4. *Effect of catalyst loading*

Fig. 12 shows influence of amount catalyst on the reaction which is the most important factor. The yield will increase as the amount of the catalyst is increased, suggesting that the availability of active sites where the transesterification reaction take place have increased. When the catalyst loading was increased from 1 to 4 wt.%, the biodiesel yield was positively increased, and the maximum FAME yield, achieved at 97% by using 5 wt.% of catalyst. Moreover, addition of an excessive amount of catalyst gives rise to the formation of an emulsion, which increases the viscosity and leads to the formation of gels, hence declining the yield of FAME (Teo et al., 2014; Taufiq-Yap et al., 2012).

## 3.9. *Reaction mechanism*

The catalytic activity toward transesterification were promoted by the presence of strong, basic sites in the catalysts that originated by the presence of $Ca^{2+}$, $Mg^{2+}$, $Sr^{2+}$ and $Ba^{2+}$. In particular, CaO was found to be very active for transesterification of vegetable oil in reflux methanol (Islam et al., 2013a; Kouzu et al., 2008). It was proposed that CaO performed transesterification reaction through a nucleophilic reaction and accelerated by the enhancement of the basic properties (Kouzu et al., 2008; Kouzu and Hidaka, 2009), as shown in Fig. 13. In the first step, CaO in transesterification reac-

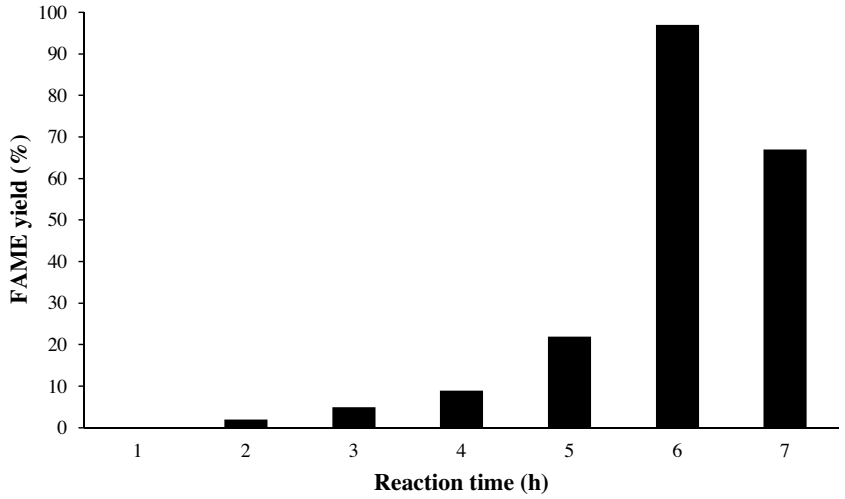


**Fig. 9 – Effect of reaction time of CS-900 catalyst on transesterification activity. Reaction conditions: palm oil 10 g, methanol:oil molar ratio 15:1, reaction temperature 65 °C and catalyst loading 5 wt.%.**

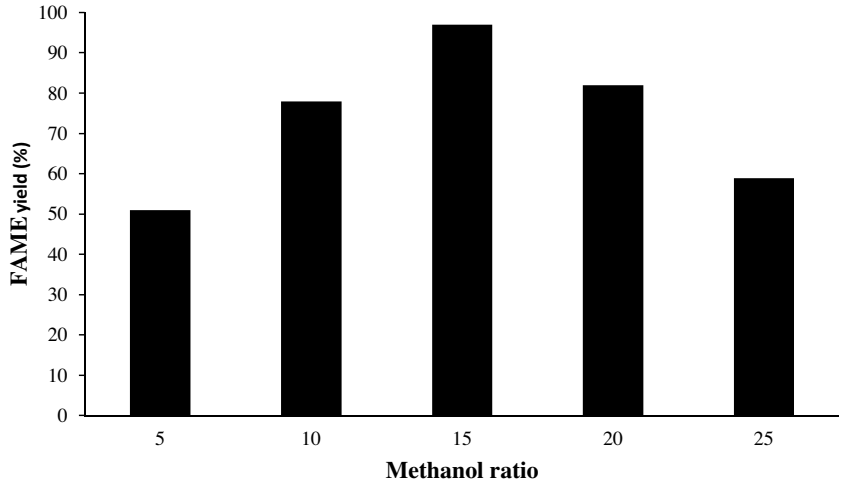


**Fig. 10 – Effect of methanol to oil molar ratio of CS-900 catalyst on transesterification activity. Reaction conditions: palm oil 10 g, catalyst amount 5 wt.%, reaction temperature 65 °C and reaction time 6 h.**

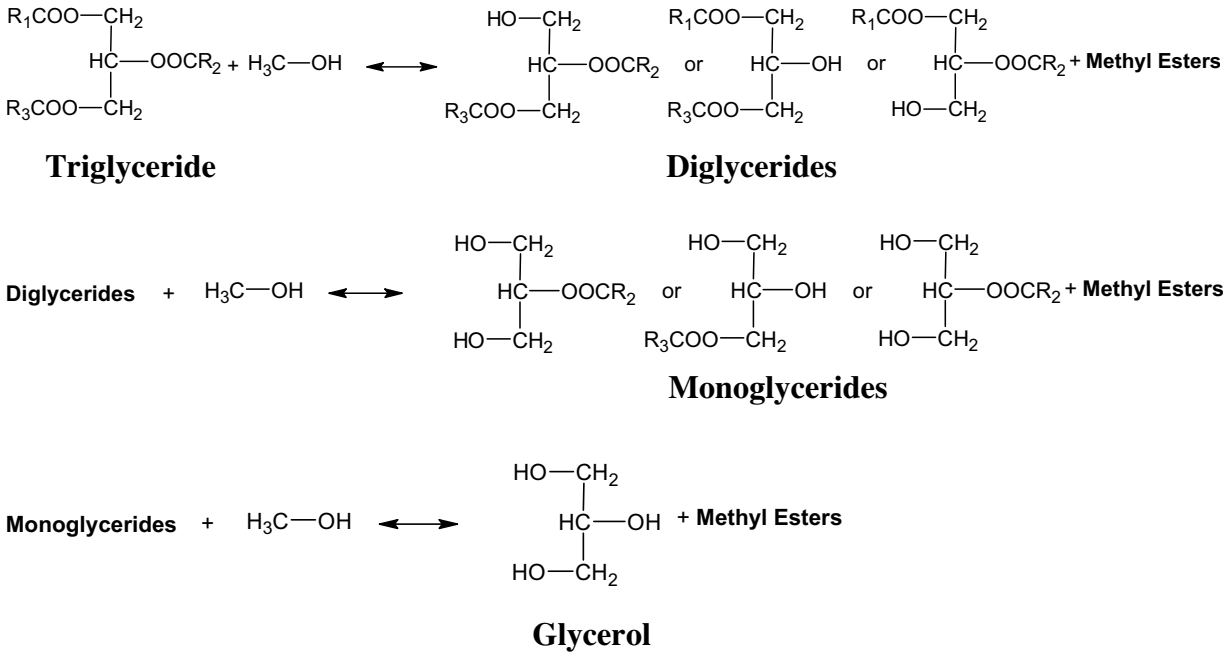


**Fig. 11 – Transesterification of representative triglyceride to methyl esters and diglycerides, monoglycerides and glycerol.**

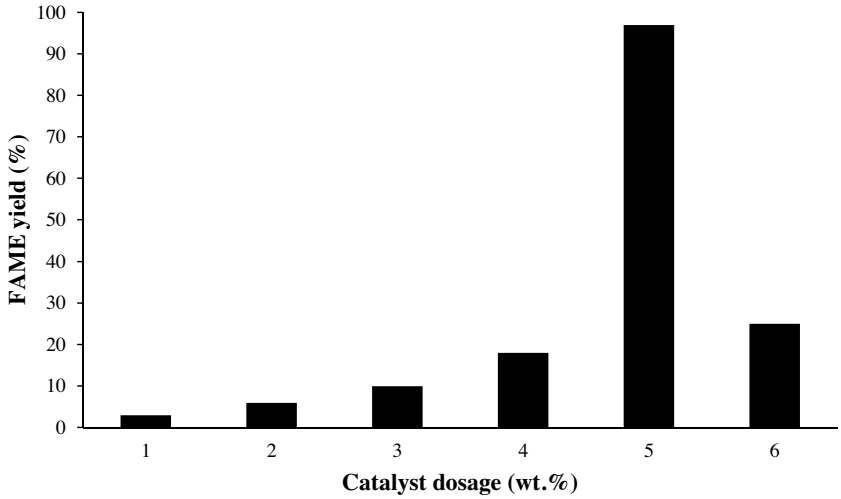


**Fig. 12 – Effect of catalyst loading of CS-900 catalyst on transesterification activity. Reaction conditions: palm oil 10 g, methanol:oil molar ratio 15:1, reaction temperature 65 °C and reaction time 6 h.**

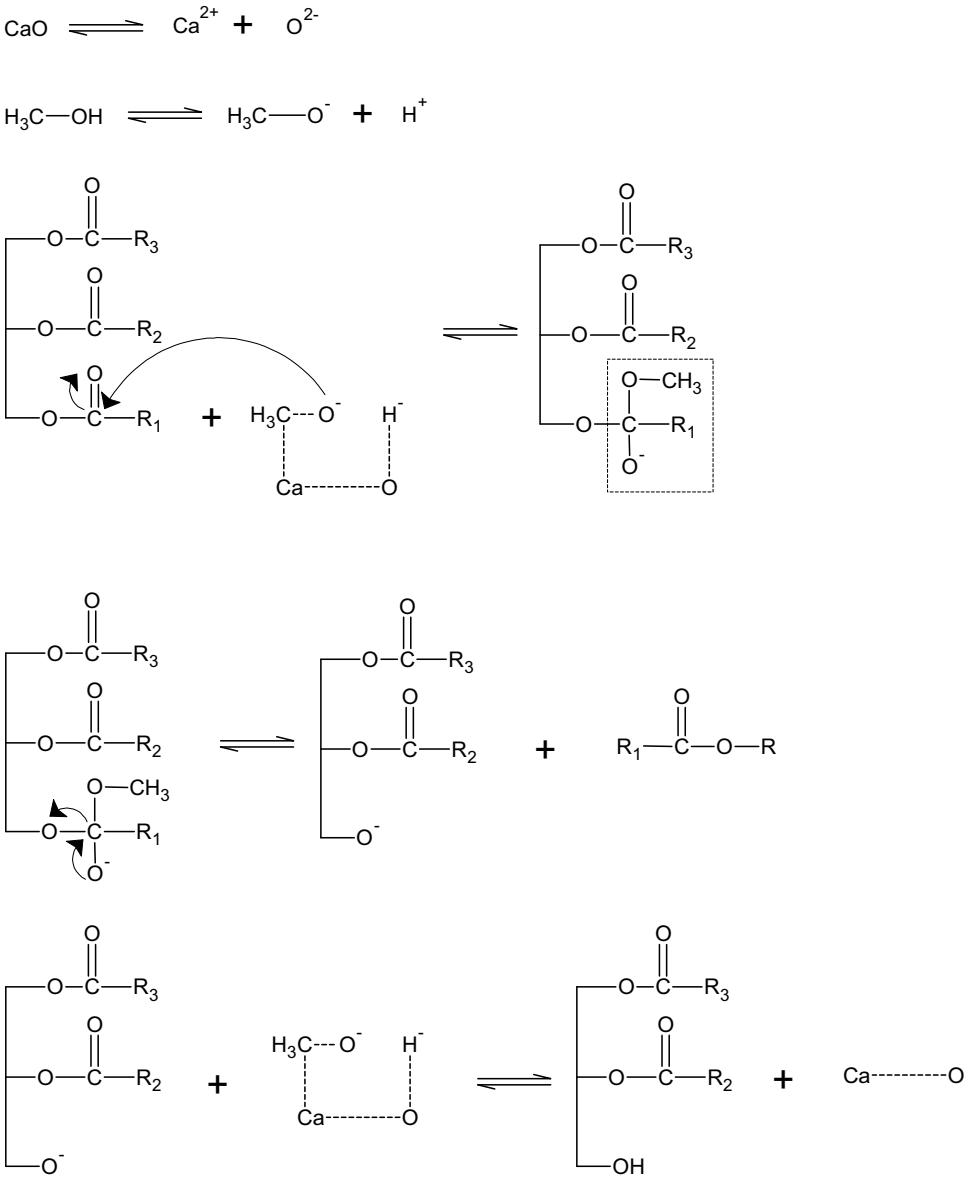


**Fig. 13 – Mechanism of CaO-catalyzed transesterification of triglyceride with methanol (Islam et al., 2013a).**

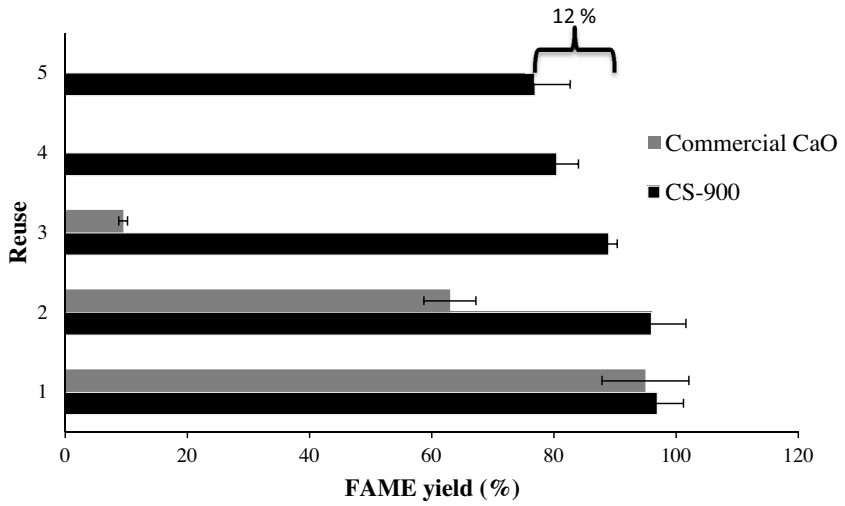


**Fig. 14 – The reusability of CS-900 and commercial CaO catalysts. Reaction conditions: palm oil 10 g, methanol:oil molar ratio 15:1, reaction temperature 65 °C and reaction time 6 h.**

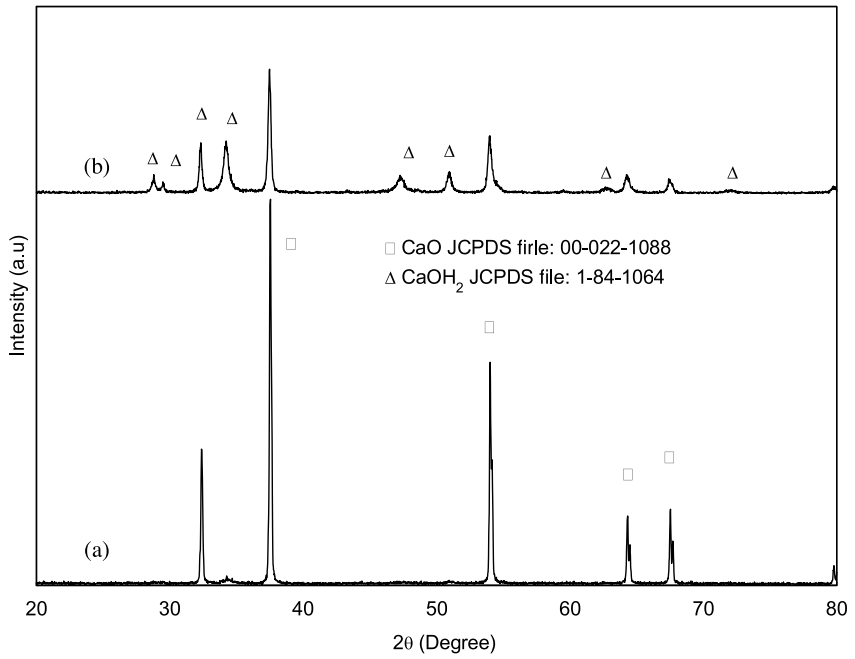


**Fig. 15 – X-ray diffraction patterns of CS-900 (a) and spent (b) catalysts. □ Characteristic peak of CaO, △ characteristic peak of $CaOH_2$ and ♦ characteristic peak of $CaCO_3$.**

tions starts with the disassociation of CaO by reacted with methanol, producing methoxide anion ($CH_3O^-$) and protonated ($H^+$) catalyst. The $CH_3O^-$ was nucleophilic attack at the carbonyl carbon of triglyceride then generated a tetrahedral intermediate (Kouzu and Hidaka, 2009). Then the rearrangement of the intermediate molecule forms a mole of methyl ester and the corresponding anion of the diglyceride. Consequently, deprotonated the catalyst to regenerate the active species that was able to react with a second molecule of methanol to start another catalytic cycle. Then, the $CH_3O^-$ will attack another carbonyl carbon atom in the resulted diglyceride, forming another mole of methyl ester and monoglyceride. Finally, the monoglyceride was converted using the same mechanism to a mixture of alkyl ester and glycerol.

### 3.10. *Reusability and leaching test of catalyst*

In order to evaluate the stability and sustainability of CS-900 catalyst, the reusability of the catalyst was further tested after the first run (Fig. 14). For each run, the catalyst was recovered by centrifugation, washing thoroughly with *n*-hexane and methanol until all traces of adhered oil and glycerol were removed, and then used for two subsequent reactions. Under the optimized condition (5 wt.% catalyst, 15:1 MeOH/oil molar ratio and 6 h), the CS-900 catalyst was able to retain sustainable 97, 96 and 86% of its activity after the 1st, 2nd and 3rd recycles, respectively. The catalyst showed good recycling ability without appreciable lost in activity. The observed drop of activity approximately 12% during regeneration and reusablility respectively at fifth cycle. The observation trend is attributed to the weight loss of catalyst during transesterification reaction and recovering the spent catalyst. Moveover, there are also weight loss on the catalyst after undergo calcination (Boro et al., 2011).

Meanwhile, commercial CaO is seen to yield lower conversion of biodiesel as compared with WVC derived catalyst. It gives about 63% yield after second cycle which lower from the first cycle which is 78%. Then, the yield significantly decreased

to about 10% of biodiesel and for the fourth cycle, there is no any conversion occured. This show that the commercial CaO has low catalytic activity compare to WVC shell derived catalyst. The deactivation was probably due to the structural changes leading to the failure to maintain the form of CaO or its transformation to other form $Ca(OH)_2$ (Fig. 15) in presence of $H_2O$ in palm oil (Boro et al., 2011). However, the catalyst can be regenerated via simple calcination. The concentration of Ca presence in biodiesel was 1.214 mg $l^{-1}$ or ppm, which is in the limit range according to EN 14214 and ASTM standards. The leaching of CaO catalyst was due to highly polar property of methanol as CaO is slightly dissolved in water (Kouzu and Hidaka, 2009).

## 4. Conclusions

In conclusion, the waste shell of *T. belcheri* has been successfully utilized as a heterogeneous catalyst in transesterification of palm oil into biodiesel. The prepared catalyst was capable of being reused for at least five times without much deterioration in the activity under the optimal condition, thus creating another low cost catalyst source for biodiesel production. Interestingly, this mild condition transesterifcation of palm oil with methanol using WVC derived CaO is promising system owing to high FAME conversion and low amount of Ca species leaching into FAME phase. The results showed the catalyst is more sustainable and high durability compare to the previous studies. Thus, the clam shell derived catalyst could stand for promising resources of low-cost and environmentally benign catalyst as it is recyclable and easily available.

## Acknowledgement

This research was supported by University Putra Malaysia and Catalysis Science and Technology Research Centre.

## References

Abdullah, A.Z., Salamatinia, B., Mootabadi, H., Bhatia, S., 2009. Energy Policy 37, 5440–5448.
Batista, I., Vidal, I., Lourenço, H.M., Sousa, I., Nunes, M.L., 1999. Eur. Food Res. Technol. 210, 31–33.
Birla, A., Singh, B., Upadhyay, S.N., Sharma, Y.C., 2012. Bioresour. Technol. 106, 95–100.
Boey, P.L., Maniam, G.P., Hamid, S.A., 2009. Bioresour. Technol. 100, 6362–6368.
Boro, J., Thakur, A.J., Deka, D., 2011. Fuel Process. Technol. 92, 2061–2092.
Cho, Y.B., Seo, G., Chang, D.R., 2009. Fuel Process. Technol. 90, 1252–1258.
Dmytryshyn, S.L., Dalai, A.K., Chaudhari, S.T., Mishra, H.K., Reaney, M.J., 2004. Bioresour. Technol. 92, 55–64.
Gnanaprakasam, A., Sivakumar, V.M., Surendhar, A., Thirumarimurugan, M., Kannadasan, T., 2013. J. Energy, 1–10, Article ID 926392.
Goldman, S., 2003. Dreaming with BRICs: The Path to to 2050. Global Economics Paper #99. Goldman Sachs, New York.
Granados, M.L., Poves, M.D.Z., Alonso, D.M., Mariscal, R., Galisteo, F.C., Moreno-Tost, R., 2007. Appl. Catal. Gen. A 73, 317–326.
Islam, A., Taufiq-Yap, Y.H., Chu, C.M., Chan, E.S., Ravindra, P., 2013a. Process Saf. Environ. Prot. 91, 131–144.
Islam, A., Taufiq-Yap, Y.H., Chu, C.H., Ravindra, P., Chan, E.S., 2013b. Renew. Energy 59, 23–29.
Juan, J.C., Kartika, D.A., Wu, T.Y., Taufiq-Yap, Y.H., 2011. Bioresour. Technol. 102 (2), 452–460.
Knothe, G., Gerpen, J., Krahl, J. (Eds.), 2005. The Biodiesel Handbook. AOCS Press, Urbana, IL, pp. 4–16.
Kouzu, M., Kasuno, T., Tajika, M., Sugimoto, Y., Yamanaka, S., Hidaka, J., 2008. Fuel 87, 2798–2806.
Kouzu, M., Hidaka, J., 2009. Fuel 93, 1–12.
Lee, D.W., Park, Y.M., Lee, K.Y., 2009. Catal. Surv. Asia 13 (2), 63–77.
Liu, X., He, H., Wang, Y., Zhu, S., Piao, X., 2008. Fuel 87 (2), 216–221.
McNeff, C.V., McNeff, L.C., Yan, B., Nowlan, D.T., Rasmussen, M., Gyberg, A.E., 2008. Appl. Catal. Gen. A 343, 39–48.
Michael, A.R., 1992. Trop. Sci. 32, 179–201.
Murugesan, A., Umarani, C., Chinnusamy, T.R., Krishnan, M., Subramanian, R., Neduzchezhain, N., 2009. Renew. Sustain. Energy Rev. 13, 825–834.
Praful, N., Singh, B., Upadhyay, S.N., Sharma, Y.C., 2012. J. Clean. Prod. 29–30, 82–90.
Sbihi, H.M., Imededdine Arbi Nehdi, I.A., Tan, C.P., Al Resayes, S.I., 2014. Energy Convers. Manag. 78, 50–57.
Sharma, Y.C., Singh, B., 2009. Renew. Sustain. Energy Rev. 13 (6–7), 1646–1651.
Sharma, Y.C., Singh, B., 2010. Fuel 89, 1470–1474.
Sharma, Y.C., Singh, B., Korstad, J., 2010a. J. Agric. Food Chem. 58, 242–247.
Sharma, Y.C., Singh, B., Korstad, J., 2010b. Energy Fuels 24, 3223–3231.
Shajaratun, Z.A., Taufiq-Yap, Y.H., Rabiah Nizah, M.F., Teo, S.H., Syazwani, O.N., Islam, A., 2014. Energy Convers. Manag. 78, 738–744.
Sieferle, R.P., 1982. The White Horse Press, Cambridge, UK.
Taufiq-Yap, Y.H., Lee, H.V., Lau, P.L., 2012. Energy Explor. Exploit. 30, 853–866.
Taufiq-Yap, Y.H., Teo, S.H., Rashid, U., Islam, A., Hussien, M.Z., 2014. Energy Convers. Manag. 88, 1290–1296.
Teo, S.H., Rashid, U., Taufiq-Yap, Y.H., 2014. Energy Convers. Manag. 87, 618–627.
Teo, S.H., Taufiq-Yap, Y.H., Rashid, U., Islam, A., 2015. RSC Adv. 5, 4266–4276.
Totarat, P., Benjapornkulaphong, S., Ngamcharussrivichai, C., Bunyakiat, K., 2006. Proceedings of the 16th Thai Chemical Engineering and Applied Chemistry Conference , Bangkok, Thailand, 26–27, p. 39.
Vicente, G., Martinez, M., Araci l, J., 2004. Bioresour. Technol. 92, 297–305.
Viriya-empikul, N., Krasae, P., Puttasawat, B., Yoosuk, B., Chollacoop, N., Faungnawakij, K., 2010. Bioresour. Technol. 101, 3765–3767.
Wei, Z., Xu, C., Li, B., 2009. Bioresour. Technol. 100, 2883–2885.
Yang, L., Zhang, A., Zheng, X., 2009. Energy Fuels 23, 3859–3865.